

# Genomic Characterization of *Ralstonia solanacearum* Phage $\phi$ RSA1 and Its Related Prophage ( $\phi$ RSX) in Strain GMI1000<sup>∇</sup>

Akiko Fujiwara, Takeru Kawasaki, Shoji Usami, Makoto Fujie, and Takashi Yamada\*

Department of Molecular Biotechnology, Graduate School of Advanced Sciences of Matter, Hiroshima University, Higashi-Hiroshima 739-8530, Japan

Received 22 July 2007/Accepted 15 October 2007

$\phi$ RSA1 is a wide-host-range bacteriophage isolated from *Ralstonia solanacearum*. In this study, the complete nucleotide sequence of the  $\phi$ RSA1 genomic DNA was determined. The genome was 38,760 bp of double-stranded DNA (65.3% G+C) with 19-bp 5'-extruding cohesive ends (*cos*) and contained 51 open reading frames (ORFs). Two-thirds of the  $\phi$ RSA1 genomic region encodes the phage structural modules, and they are very similar to those reported for coliphage P2 and P2-like phages. A  $\phi$ RSA1 minireplicon with an 8.2-kbp early-expressing region was constructed. A late-expression promoter sequence motif was predicted for these  $\phi$ RSA1 genes as 5' TGTTGT-(X)<sub>13</sub>-ACAACA. The genomic sequence similarity between  $\phi$ RSA1 and related phages  $\phi$ S2237 and  $\phi$ CTX was interrupted by three AT islands, one of which contained an insertion sequence element, suggesting that they were recombinational hot spots.  $\phi$ RSA1 was found to be integrated into at least three different strains of *R. solanacearum*, and the chromosomal integration site (*attB*) was identified as the 3' portion of the arginine tRNA(CCG) gene. In the light of the  $\phi$ RSA1 gene arrangement, one possible prophage sequence previously detected on the chromosome of *R. solanacearum* strain GMI1000 was characterized as a  $\phi$ RSA1-related prophage (designated  $\phi$ RSX).  $\phi$ RSX was found to be integrated at the serine tRNA (GGA) gene as an *att* site, and its size was determined to be 40,713 bp.  $\phi$ RSX ORFs shared very high amino acid identity with their  $\phi$ RSA1 counterparts. The relationships and evolution of these P2-like phages are discussed.

*Ralstonia solanacearum* is a soil-borne gram-negative bacterium known to be the causative agent of bacterial wilt in many important crops (20, 51). This bacterium has an unusually wide host range, with more than 200 species belonging to more than 50 botanical families (21). *R. solanacearum* strains represent a heterogeneous group subdivided into five races on the basis of their host range or six biovars based on their physiological and biochemical characteristics (21). Recently, the complete genome sequence of *R. solanacearum* GMI1000 was reported (44). The 5.8-Mbp genome consists of two replicons, a 3.7-Mbp chromosome and a 2.1-Mbp megaplasmid. Such a bipartite genome structure seems to be a characteristic of *R. solanacearum*, as a megaplasmid has been detected in most of the strains of this species (42). Both replicons of strain GMI1000 contain a number of regions known as alternative codon usage regions (ACURs), most of which differ significantly in G+C content from the average of 67% found in the entire genome, with G+C contents varying from 50% to 70%. These regions are often associated with mobile genetic elements such as prophages, insertion sequences (ISs), and IS-related sequences, suggesting that ACURs may have been acquired through horizontal gene transfer and have an important role in genomic evolution (44). At least four possible prophage sequences were detected on the chromosome of strain GMI1000, but the nature of these is largely unknown.

Recently, Yamada et al. (52) detected and isolated various kinds of bacteriophage that specifically infect *R. solanacearum* strains belonging to different races and/or biovars. Two of the

phages,  $\phi$ RSS1 and  $\phi$ RSM1, are filamentous Ff-like phages (inoviruses) and contained single-stranded DNA genomes of 6,662 and 9,004 bases, respectively (30). Both phages have an integrative nature, and some strains of *R. solanacearum* contained prophages of these at a specific *att* sequence.  $\phi$ RSL1, another phage, with a head-tail structure resembling that of phages belonging to the myoviruses, contained an approximately 240-kb double-stranded DNA genome. This phage has a wider host range and only replicates via a lytic cycle. A template phage,  $\phi$ RSA1, spontaneously appeared from a strain of *R. solanacearum* (MAFF211272) and showed the widest host range; all of the strains tested, including those of races 1, 3, and 4 and biovars 3, 4, and N2, produced plaques on assay plates.  $\phi$ RSA1 particles have a unique morphology with a head and a tail, to the bottom of which a tail sheath is connected. A similar structure was also reported for *Burkholderia cepacia* phage KS5 (46). The genome of  $\phi$ RSA1 is a 39-kb linear DNA. A lysogenic state of this kind of phage was detected by genomic Southern blot analysis in 3 of 15 strains of the different races and different biovars (52).

In this study, the complete nucleotide sequence of the  $\phi$ RSA1 genomic DNA was determined. In the light of the  $\phi$ RSA1 gene arrangement, one possible prophage sequence previously detected on the chromosome of *R. solanacearum* strain GMI1000 was characterized as a  $\phi$ RSA1-related prophage (designated  $\phi$ RSX).

## MATERIALS AND METHODS

**Bacterial strains and phages.** Wild-type *R. solanacearum* strains M4S and MAFF106611 and strain MAFF211272 were from the Leaf Tobacco Research Center, Japan Tobacco Inc., and the National Institute of Agrobiological Sciences, Japan, respectively. Bacterial cells were cultured in CPG medium (26) at 28°C with shaking at 200 to 300 rpm. Phages were propagated and purified from

\* Corresponding author. Mailing address: Department of Molecular Biotechnology, Graduate School of Advanced Sciences of Matter, Hiroshima University, 1-3-1 Kagamiyama, Higashi-Hiroshima 739-8530, Japan. Phone and fax: 81-82-424-7752. E-mail: tayamad@hiroshima-u.ac.jp.

<sup>∇</sup> Published ahead of print on 26 October 2007.

TABLE 1.  $\phi$ RSA1-specific oligonucleotide primers used for cloning and plasmid construction

Oligonucleotide primer	Sequence (5' to 3') <sup>a</sup>	Location (nt) <sup>b</sup>
attP-L <sup>c</sup>	GCAGTATGTGTCCTGGGTGTTTGTCTACCG	36488–36517
attP-R <sup>c</sup>	CCTCTTATCAGAACGCCCACTCC	37203–37178
ORF33-P1	GATCCAGCCGGAGAAGTTGGAAGAATCGGG	25247–25276
ORF36-P2	GCGAGCCGGTCTCCGTAGTGCATTTTCAAT	28000–28029
ORF39-P3	CTCTTCCCCTCACGTTTTTTTCGCGCCTTG	28997–29026
ORF49-P4	AGAGCGACAAAGCTTGATTTCTTTGCTTG	35718–35689
ORF35-P5	GTTCAGGCTCACGGAATCTTCGAAGAACC	27485–27514

<sup>a</sup> Sequence underlined is changed to a HindIII site.

<sup>b</sup> Numbering corresponds to the sequence with DDBJ accession no. AB276040.

<sup>c</sup> A 720-bp region containing attP of  $\phi$ RSA1 was amplified with these primers and used as a probe to confirm the exact integration of  $\phi$ RSA1 in strain MAFF211272 by genomic Southern blot analysis.

single-plaque isolates. Routinely, the  $\phi$ RSA1 phage was propagated by using strain M4S as the host. A 16- to 24-h culture of bacterial cells grown in CPG medium was diluted 100-fold with 100 ml fresh CPG medium in a 500-ml flask. To collect sufficient amounts of phage particles, a total of 2 liters of bacterial culture was grown. When the cultures reached 0.2 U of optical density at 600 nm, the phage was added at a multiplicity of infection of 0.001 to 1.0. After further growth for 9 to 18 h, the cells were removed by centrifugation with an R12A2 rotor in a Hitachi himac CR21E centrifuge at 8,000  $\times$  g for 15 min at 4°C. To increase phage recovery, EGTA (to a final concentration of 1 mM) was added to the  $\phi$ RSA1-infected culture at 6 to 9 h postinfection. The supernatant was passed through a 0.2- $\mu$ m-pore-size membrane filter, and phage particles were precipitated by centrifugation with a P28S rotor in a Hitachi XII100 $\beta$  centrifuge at 40,000  $\times$  g for 1 h at 4°C and dissolved in SM buffer (50 mM Tris-HCl at pH 7.5, 100 mM NaCl, 10 mM MgSO<sub>4</sub>, 0.01% gelatin). Purified phages were stained with Na-phosphotungstate before observation in a Hitachi H600A electron microscope as described by Yamada et al. (52).  $\lambda$  phage particles were used as an internal standard marker for size determination. *Escherichia coli* XL10 Gold and pBluescript II SK+ were obtained from Stratagene (La Jolla, CA).

**DNA manipulations and sequencing.** Standard molecular biological techniques for DNA isolation, digestion with restriction enzymes and other nucleases, and construction of recombinant DNAs were followed as described by Sambrook and Russell (45). Phage DNA was isolated from purified phage particles by phenol extraction. In some cases, purified phage particles were embedded in 0.7% low-melting-point agarose (InCert agarose; FMC Corp.). After treatment with proteinase K (1 mg/ml; Merck) and 1% Sarkosyl, it was subjected to pulsed-field gel electrophoresis with a CHEF MAPPER electrophoresis apparatus (Bio-Rad) as described by Higashiyama and Yamada (24). Shotgun cloning and sequencing were performed at Hitachi High-Tech Fields Corp. as follows.  $\phi$ RSA1 whole genomic DNA was fragmented by sonication. DNA fragments in the ~2-kb range were blunt ended and cloned with the pTS1/HincII vector (NipponGene) in *E. coli* cells. Shotgun sequencing of the clones (with an averaged insert of 2.0 kb) was performed with a BigDye Terminator version 3.1 cycle sequencing kit (Applied Biosystems) in an Applied Biosystems 3700 DNA analyzer. A total of 920 sequences larger than 150 bases were assembled by the use of a phred/phrap/consed program (<http://www.phrap.org>). The analyzed sequences corresponded to 6.0 times the final genome size of 38,760 bp. Potential open reading frames (ORFs) larger than 300 bp were identified by using the online program Orfinder (<http://www.ncbi.nlm.nih.gov/gorf/gorf.html>) and the DNASIS program (version 3.6; Hitachi Software Engineering Co. Ltd.). To assign possible functions to ORFs, searches through the databases were performed with the BLAST, BLASTX, and BLASTP programs (1).

To identify the attP and attB sequences of  $\phi$ RSA1, genomic DNA of  $\phi$ RSA1 lysogenic strain MAFF211272 of *R. solanacearum* was digested with HincII and hybridized with a  $\phi$ RSA1 DNA probe as described below. Two hybridizing bands of 2.6 and 5.7 kbp which possibly contain each of the integration junctions were cut out from the gel, ligated to the EcoRV site of pBluescript II SK+, and cloned in *E. coli* XL10 Gold. The nucleotide sequences determined for the clones were compared with the  $\phi$ RSA1 genomic sequence.

An autonomously replicating plasmid (minireplicon) was constructed from  $\phi$ RSA1 DNA as follows. Regions on the right side of the  $\phi$ RSA1 genome which contain possible early genes, including those for DNA replication, were amplified by PCR with a combination of forward primers (ORF33-P1, ORF36-P2, ORF39-P3, and ORF35-P5; Table 1) and reverse primer ORF49-P4 (Table 1). Twenty-five rounds of PCR were performed with 1 ng of  $\phi$ RSA1 DNA as the template under standard conditions in an MY Cyclor (Bio-Rad). After digestion with

HindIII at the reverse primer sites, the amplified fragment was connected to a Km<sup>r</sup> cassette cut out with HindIII and SmaI from plasmid pUC4-KIXX (Amersham Biosciences). It was then introduced into cells of strains M4S and MAFF106611 by electroporation with a Gene Pulser Xcell (Bio-Rad) with a 2-mm cell at 2.5 kV in accordance with the manufacturer's instructions. Transformants were selected on CPG plates containing 15  $\mu$ g/ml kanamycin (Meiji Seika, Tokyo, Japan).

**Southern blot hybridization.** Genomic DNA of *R. solanacearum* cells was prepared by the miniprep method as described by Ausubel et al. (2). After digestion with various restriction enzymes, DNA fragments were separated by agarose gel electrophoresis, blotted onto a nylon membrane (Biodyne, Pall Gelman Laboratory, Closter, NJ), hybridized with a probe ( $\phi$ RSA1 genomic DNA) labeled with fluorescein (Gene Images random prime labeling kit; Amersham Biosciences, Uppsala, Sweden), and detected with a Gene Images CDP-Star detection module (Amersham Biosciences). Hybridization was performed in a buffer containing 5 $\times$  SSC (1 $\times$  SSC is 0.15 M NaCl plus 0.015 M sodium citrate), 0.1% sodium dodecyl sulfate (SDS), 5% liquid block, and 5% dextran sulfate for 16 h at 65°C. The filter was washed at 60°C in 1 $\times$  SSC–0.1% SDS for 15 min and then in 0.5 $\times$  SSC–0.1% SDS for 15 min with agitation, in accordance with the manufacturer's protocol. The hybridization signals were detected by exposing the filter to X-ray film (RX-U; Fuji Film, Tokyo, Japan).

**In planta virulence assay of *R. solanacearum* strains.** Cells of *R. solanacearum* were grown in CPG medium for 1 to 2 days at 28°C. After centrifugation, cells were resuspended in distilled water at a density of 10<sup>8</sup>/ml. The cell suspension was injected with a needle into the major stem of tobacco plants (*Nicotiana tabacum* SR1, 4 weeks old with four to six leaves) at a site 1 cm above the soil level (just above the cotyledons). As a control, distilled water was injected in the same manner. Each bacterial strain was injected into five plants. Plants were cultivated in a Sanyo Growth Cabinet (Sanyo, Osaka, Japan) at 25°C (16 h light, 8 h dark) for 3 to 4 weeks before detailed examination. Symptoms of wilting were graded from 1 to 5 as described by Winstead and Kelman (50). Extracellular polysaccharide production by *R. solanacearum* cells was assayed by the method of Gatt and Berman (15).

**Nucleotide sequence accession number.** The  $\phi$ RSA1 genomic sequence was deposited in DDBJ under accession no. AB276040.

## RESULTS AND DISCUSSION

**Host range and lysogenic nature of  $\phi$ RSA1.**  $\phi$ RSA1 has a wide host range; all 15 strains of the different races or biovars of *R. solanacearum* produced plaques (with variable frequency) on assay plates (52). With strain M4S as the host,  $\phi$ RSA1 titers were usually not so high; a value of 2  $\times$  10<sup>8</sup> to 1  $\times$  10<sup>9</sup> PFU/ml was obtained, but phage recovery was dramatically increased (100-fold) by addition of 1 mM EGTA to the  $\phi$ RSA1-infected host culture. This EGTA effect was also reported for  $\phi$ CTX, which uses the lipopolysaccharide core as a receptor site on the cell surface and requires Ca<sup>2+</sup> ions for binding to the receptor (38). In that case, EGTA treatment reduced phage adsorption, and when the phage was added at the final stage of infection, its recovery from the cell debris greatly increased. On the basis of these sim-

TABLE 2. Predicted ORFs found in the RSA1 genome

Coding sequence	Position (5' to 3')	G+C content (%)	Protein length (aa)	Mol. mass (Da)	Amino acid sequence identity/similarity to best homologs	BLAST score (E value)	Accession no.
ORF1	353–742	65.9	130	13,173	<i>Janthinobacterium lividum</i> hypothetical protein	113 (3e-24)	A1X1P8
					PAAR motif protein ( <i>Burkholderia multivorans</i> )	82 (1e-14)	A0UPR0
ORF2	747–1247	68.9	167	18,701	<i>Janthinobacterium lividum</i> hypothetical protein	168 (8e-41)	A1X1P7
ORF3	1260–2189	68.1	310	33,466	<i>Burkholderia thailandensis</i> hypothetical protein	79 (3e-13)	Q2SWS5
ORF4	2102–2914	65.5	271	30,022	<i>Janthinobacterium lividum</i> hypothetical protein	176 (1e-42)	A1X1P4
ORF5	4008–2905	65.4	368	41,541	Bacteriophage protein RSc1941	642 (0.0)	Q8XY22
					Bacteriophage P2 gpQ probable capsid portal protein	396 (e-109)	P25480
ORF6	5786–4008	65.3	593	67,089	Terminase RSc1939 (ATPase subunit-related protein)	707 (0.0)	Q8XY24
					Putative ATPase subunit of terminase (gpP)	504 (e-141)	Q8Z358
					Bacteriophage P2 gpP	431 (e-119)	P25479
ORF7	5922–6764	65.2	281	30,415	Bacteriophage protein RSc1938	461 (e-128)	Q8XY25
					Phage capsid scaffolding protein (gpO)	201 (4e-50)	Q2T5K2
					Bacteriophage P2 gpO	192 (2e-47)	P25478
ORF8	6821–7837	63.5	339	37,784	Bacteriophage protein RSc1937	537 (e-151)	Q8XY26
					P2 family phage major capsid protein (gpN)	382 (e-104)	Q45YE6
					Bacteriophage P2 gpN	346 (8e-94)	P25477
ORF9	7837–8556	68.0	240	26,476	Bacteriophage protein RSc1936	439 (e-122)	Q8XY27
					Terminase, endonuclease subunit (gpM)	180 (5e-44)	P25476
ORF10	8656–9132	70.0	159	17,076	Bacteriophage protein RSc1935	322 (5e-87)	Q8XY28
					Head completion/stabilization protein L (gpL)	120 (3e-26)	P25475
ORF11	9135–9338	72.1	68	7,307	Bacteriophage protein RSc1934	138 (1e-31)	Q8XY29
					Phage tail X (gpX)	91 (2e-17)	Q41S37
ORF12	9357–9758	70.6	134	13,018	Phage-related transmembrane protein RSc1933	179 (5e-44)	Q8XY30
ORF13	9758–10069	70.7	104	11,253	Phage-related transmembrane protein RSc1932	173 (3e-42)	Q8XY31
					Putative holin	50 (3e-05)	A1AE02
ORF14	10069–10872	70.1	268	28,697	Phage-related protein (hydrolase) RSc1931	500 (e-140)	Q8XY32
					Phage-encoded peptidoglycan-binding protein	290 (5e-77)	A0UZD9
					Bacteriophage $\phi$ CTX ORF11	249 (8e-65)	Q92XL6
ORF15	10872–11366	67.5	165	17,049	Signal peptide protein RSc1930	169 (6e-41)	Q8XY33
ORF16	11366–11797	67.4	144	16,042	Tail completion-like protein RSc1929	286 (2e-76)	Q8XY34
					Bacteriophage P2 gpR	126 (3e-28)	P36933
ORF17	11797–12240	68.0	148	16,679	Tail completion-like protein RSc1928	170 (2e-41)	Q8XY35
					Bacteriophage P2 tail completion protein gpS	67 (4e-10)	P36934

Continued on following page

TABLE 2—Continued

Coding sequence	Position (5' to 3')	G+C content (%)	Protein length (aa)	Mol. mass (Da)	Amino acid sequence identity/similarity to best homologs	BLAST score (E value)	Accession no.
ORF18	13153–12215	45.6	313	36,444	<i>Burkholderia pseudomallei</i> hypothetical protein	189 (1e-46)	Q6S459
ORF19	13397–14011	69.2	205	21,753	Phage-related protein RSc1925 (baseplate assembly-like protein)	384 (e-105)	Q8XY38
					Baseplate assembly protein V (gpV)	160 (3e-38)	A0UFJ5
					Bacteriophage P2 gpV	108 (2e-22)	P31340
ORF20	14011–14355	69.4	115	12,612	Phage-related protein RSc1924 (baseplate assembly-like protein)	216 (3e-55)	Q8XY39
					gpW/gp25 family protein	124 (1e-27)	A0U2D3
					Bacteriophage P2 gpW	89 (9e-17)	P51768
ORF21	14361–15266	69.8	302	32,456	Baseplate assembly-like protein RSc1923	517 (e-145)	Q8XY40
					Baseplate J-like protein (gpJ)	320 (8e-86)	Q1QXR7
					Bacteriophage P2 gpJ	317 (5e-85)	P51767
ORF22	15262–15876	70.4	205	22,168	Tail-related protein RSc1922	370 (e-101)	Q8XY41
					Phage tail protein gpI (tail formation-like protein)	227 (2e-58)	Q1QXR8
					Bacteriophage P2 gpI	216 (4e-55)	P26701
ORF23	15884–17545	70.8	554	57,813	Tail fiber-related protein RSc1921	951 (0.0)	Q8XY42
					Tail fiber protein gpH	269 (3e-70)	Q87ZM6
					Bacteriophage P2 gpH	148 (9e-34)	P26700
ORF24	16871–17545	67.8	225	23,947	Phage tail fiber protein RSc1692	108 (2e-22)	Q8XYR6
ORF25	17561–18310	72.8	250	25,888	Tail fiber assembly-like protein RSc1920	362 (7e-99)	Q8XY43
ORF26	18310–18771	68.8	154	17,140	Hypothetical protein RSc1919	259 (2e-68)	Q8XY44
ORF27	18868–20040	67.7	391	42,397	Phage-related tail sheath protein RSc1918	758 (0.0)	Q8XY45
					P2 major tail sheath protein gpFI	585 (e-165)	Q66BD0
					Bacteriophage P2 gpFI	510 (e-143)	P22501
ORF28	20075–20581	62.5	169	18,802	Phage-related protein (major tail protein) RSc1917	341 (7e-93)	Q8XY46
					Putative P2 tail tube protein gpFII	174 (1e-42)	Q66BD1
					Bacteriophage P2 gpFII	147 (2e-34)	P22502
ORF29	20630–20983	63.2	118	12,796	Phage-related protein RSc1916	225 (5e-58)	Q8XY47
					Bacteriophage P2 gpE	83 (5e-15)	Q66BM8
ORF30	21081–23657	69.6	859	90,965	Phage-related tail transmembrane protein RSc1914	1,280 (0.0)	Q8XY49
					Bacteriophage P2 tail protein gpT	109 (6e-22)	Q66BN0
ORF31	23749–24168	65.2	140	15,695	Phage-related tail protein RSc1913	281 (7e-75)	Q8XY50
					Bacteriophage P2 gpU	155 (5e-37)	Q41SZ1
ORF32	24168–25370	66.2	401	43,433	Phage related protein RSc1912	669 (0.0)	Q8XY51
					Bacteriophage P2 gpD	322 (3e-86)	Q66BD6
ORF33	26135–25392	61.8	248	26,462	Hypothetical transmembrane protein	134 (4e-30)	Q8XSE3
ORF34	27434–26217	62.6	406	47,730	Transposase ISRSO15	803 (0.0)	Q8XFK1
ORF35	28022–27609	59.9	138	15,091	XRE family, transcriptional regulator	103 (2e-21)	A0UFH8
					Putative phage DNA-binding protein	102 (6e-21)	Q63YP6
					DNA-binding repressor RSc1907	99 (7e-20)	Q8XY56

Continued on facing page

TABLE 2—Continued

Coding sequence	Position (5' to 3')	G+C content (%)	Protein length (aa)	Mol. mass (Da)	Amino acid sequence identity/similarity to best homologs	BLAST score (E value)	Accession no.
ORF36	28062–28490	59.7	143	15,823	Unknown		
ORF37	28539–28730	58.3	64	7,380	Unknown		
ORF38	28730–28975	66.5	82	9,126	Putative transcription activator RSc1904 Phage transcription activator Ogr/Delta	124 (2e-27) 77 (4e-13)	Q8XY59 A0UFH5
ORF39	29093–29644	65.9	184	20,512	Hypothetical phage protein Prophage antirepressor	235 (9e-61) 95 (1e-18)	Q63YQ0 Q3R0Y7
ORF40	29657–29887	61.9	77	8,082	Hypothetical protein RSc1903	75 (1e-12)	Q8XY60
ORF41	29887–30048	65.8	54	5,540	Hypothetical protein RSc1902	81 (1e-14)	Q8XY61
ORF42	30048–30251	63.4	68	7,171	Transmembrane protein RSc1901	58 (2e-07)	Q8XY62
ORF43	30254–30487	64.5	78	8,612	Transmembrane protein Rsc1900	147 (2e-34)	Q8XY63
ORF44	30483–30692	70.0	70	7,810	Hypothetical protein RSc1899	103 (3e-21)	Q8XY64
ORF45	30770–31243	65.5	158	17,212	Unknown		
ORF46	31512–31799	65.3	96	11,432	<i>Pseudomonas resinovorans</i> /pCAR1 ORF80	128 (1e-28)	Q8GHW9
ORF47	31802–34603	65.6	934	103,175	Zinc finger, CHC family protein $\phi$ 52237 hypothetical protein (AAZ72605.1) Conserved hypothetical phage protein	1,454 (0.0) 1437 (0.0) 1,433 (0.0)	A0UFH0 Q45Y14 Q63YQ8
ORF48	33589–31811	66.4	593	63,364	Hypothetical protein $\phi$ 52237 (AAZ72604.1)	332 (1e-80)	Q45Y15
ORF49	34778–35494	61.7	239	25,241	Unknown		
ORF50	35709–36788	64.3	360	41,524	Site-specific recombinase, phage integrase	514 (e-144)	Q62FM0
tRNA	36831–36875	71.1			<i>attP</i> [Arg tRNA(CCG)] <i>R. solanacearum</i> GMI1000 chromosomal sequence	90 (7e-17)	AL646073
ORF51	37124–38182	56.4	353	38,895	Unknown		

ilar observations, we suspect that the lipopolysaccharide receptor and  $\text{Ca}^{2+}$  ions are involved in the adsorption of  $\phi$ RSA1 to *R. solanacearum*.

$\phi$ RSA1 spontaneously appeared from strain MAFF211272 (52), but UV light irradiation of this strain did not induce phage production; the lysates prepared by UV irradiation contained a rather reduced number of infectious phage particles compared with the culture supernatant of untreated cells ( $3.7 \times 10^3$  PFU/ml without UV irradiation and  $3.4 \times 10^3$  PFU/ml with UV irradiation for 16 s). This result indicated that  $\phi$ RSA1 is not UV inducible.

**Determination of the genomic DNA sequence.** In our previous study, the  $\phi$ RSA1 genomic DNA gave a ladder pattern of a 39-kbp unit by pulsed-field gel electrophoresis (52), indicating a linear molecule of 39 kbp. To determine the nucleotide sequence of the entire  $\phi$ RSA1 genomic DNA, shotgun cloning

and sequencing were performed (as described in Materials and Methods). A total of 920 sequences larger than 150 bases were assembled by the use of the Phred/Phrap/Consed program. The analyzed sequences corresponded to 6.0 times the final genome size of 38,760 bp. The  $\phi$ RSA1 genome has a G+C content of 65.3%. Potential ORFs that consist of more than 100 codons and start with ATG or GTG were identified with the online program Orfinder and the DNASIS program (version 3.6; Hitachi Software Engineering Co. Ltd.). To assign possible functions to ORFs, searches through the databases were done with the BLAST, BLASTX, and BLASTP programs (1). When two ORFs in different reading frames overlapped, the ORFs that had homologies to known sequences or a codon usage typical of the host *R. solanacearum* were selected. Accordingly, a total of 51 potential ORFs were assigned on the genome (Table 2 and Fig. 1). Most ORFs started with ATG



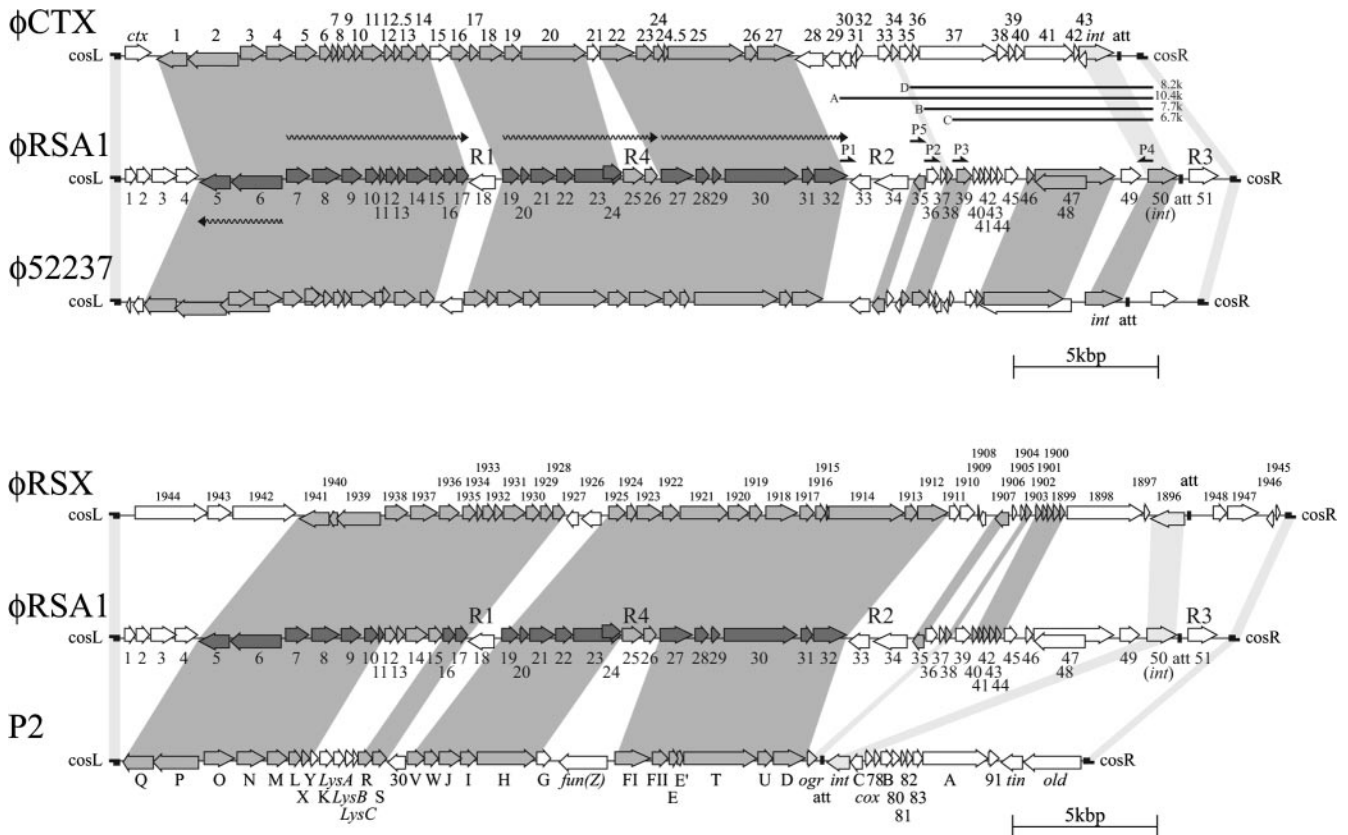


FIG. 1. (Top) Alignment of  $\phi$ RSA1 ORFs with those of  $\phi$ CTX (38) and  $\phi$ 52237 (accession no. DQ087285). (Bottom) Alignment of  $\phi$ RSA1 ORFs with those of P2 (GenBank accession no. NC001895) and a prophage (designated  $\phi$ RSX in this work) previously found in the genome of *R. solanacearum* GMI1000 (9, 44). ORFs are indicated by arrows. Predicted transcription units for  $\phi$ RSA1 late genes are shown by wavy lines. Gray shading indicates significant amino acid or nucleotide sequence similarity among the phages. Light gray shading indicates marginally similar regions. R1, R2, R3, and R4 are regions with relatively low G+C contents (AT-rich regions), corresponding to ACURs (44). P1, P2, P3, P5, and P4 are PCR primers for minireplicon formation. A, B, C, and D are fragments of 10.4, 7.7, 6.7, and 8.2 kbp, respectively, used for minireplicon formation.

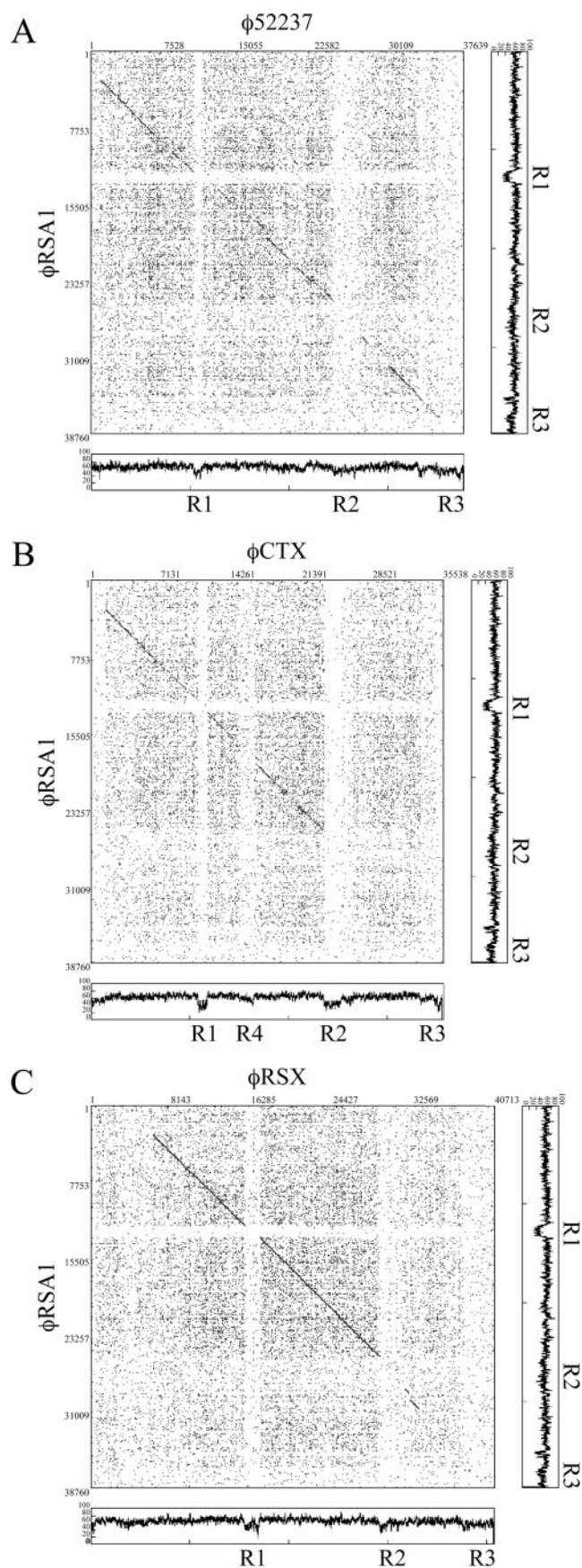
and ended with TGA, but five ORFs (based on the database sequence) started with GTG (ORF13, -20, -22, -24, and -32). Five ORFs ended with TAA (ORF2, -22, -28, -43, and -46), and four ORFs ended with TAG (ORF17, -21, -26, and -36). In two cases, extended overlapping of two ORFs was observed, i.e., ORF23 and -24 and ORF47 and -48. As indicated in Table 2, in each case, significant homology was detected for each ORF in the database and so they are included in the final assignment.

**$\phi$ RSA1 gene organization and homology to other phage genomes.** The databases were searched with the BLAST and BLASTX programs for sequences homologous to the nucleotide sequence of  $\phi$ RSA1 DNA. Extensive homologies were detected in the genomic sequences of *Burkholderia pseudomallei* phage  $\phi$ 52237 (accession no. DQ087285), *Pseudomonas aeruginosa* phage  $\phi$ CTX (accession no. AB008550), and coliphage P2 (accession no. AF063097) and the chromosomal DNA of *R. solanacearum* GMI1000 (accession no. AL646052).

To avoid confusion, the P2 definition of the genes was followed in the identification of  $\phi$ RSA1 genes in this study. Interestingly, *R. solanacearum* was formerly classified as *Pseudomonas solanacearum* and had another synonym, *Bacillus solanacearum* (47, 51), based on classical taxonomic character-

istics. Currently, the three bacterial genera *Ralstonia* (*Beta*-*proteobacteria*), *Burkholderia* (*Betaproteobacteria*), and *Pseudomonas* (*Gammaproteobacteria*) are clearly distinguished from each other on the basis of their 16S rRNA sequences (51). In this context, we are interested in the interrelationships among the three phages  $\phi$ RSA1,  $\phi$ CTX, and  $\phi$ 52237.

Extended comparison of the  $\phi$ RSA1 sequence with these sequences by the matrix plot method revealed characteristic features of the phage gene organization, as shown in Fig. 2. Between the  $\phi$ RSA1 and  $\phi$ 52237 (37,639 bp) sequences, an extended colinearity was obvious throughout almost the entire genomic region (Fig. 2A). The sequence homology was broken by three small regions around  $\phi$ RSA1 positions 12,500 to 13,500 (region R1), 26,000 to 29,000 (region R2), and 37,000 to 38,760 (region R3), whose G+C contents were 50.5% (region R1), 60.6% (region R2), and 56.1% (region R3) and relatively low compared with the overall average value of the genome (65.3%). These regions with low G+C contents (AT islands) correspond to  $\phi$ 52237 positions 10,000 to 12,000 (58.6% G+C), 24,000 to 27,000 (57.3% G+C), and 35,600 to 37,630 (53.1% G+C), whose G+C contents are also lower than the overall average value of the  $\phi$ 52237 genome (64.8%). In the comparison between  $\phi$ RSA1 and  $\phi$ CTX, colinearity was lim-



ited to the initial two-thirds of the genomes (Fig. 2B). Interestingly, the sequence homology was broken by the same AT islands of the  $\phi$ RSA1 genome. On the  $\phi$ CTX genome (35,652 bp), regions R1 to R3 approximately corresponded to positions 10,500 to 12,000 (51% G+C), 23,500 to 25,500 (46.2% G+C), and 35,000 to 35,652 (47.1% G+C). In addition, another break was seen around positions 15,000 to 16,500 (58.0% G+C; region R4). The G+C contents of these  $\phi$ CTX regions are again lower than the average genomic G+C content of 62.6%. In each comparison, these AT islands can be recognized as blank lattices against a background of dotted areas, suggesting that they are regions containing unrelated sequences probably acquired recently.

$\phi$ RSA1 region R1 corresponds to a region containing ORF18 (function unknown) between structural genes *gpS* (*orf17*) and *gpV* (*orf19*). In the same location,  $\phi$ CTX contains ORF15 (function unknown). Region R2 of  $\phi$ RSA1 corresponds to the junction where the homology with  $\phi$ CTX ends. This AT island of approximately 3.0 kb separates the *gpD* gene (*orf32*) and the *ogr* gene (*orf38*), which are immediately linked to each other on the coliphage P2 genome. A similar AT island of 3.4 kb was found to be inserted in the same region in  $\phi$ CTX, where six ORFs with unknown functions are located (38). These ORFs showed no homology with any of five ORFs (ORF33 to -37) in  $\phi$ RSA1 region R2. It is interesting that ORF34, located close to ORF32 (the *gpD* homologue), showed 100% amino acid sequence identity with transposase ISRSO15, which was found in the chromosomal DNA (positions 2,780,153 to 2,781,370; accession no. AL646070), as well as the megaplasmid DNA (positions 111,895 to 113,185; accession no. AL646085) of *R. solanacearum* GMI1000. ORF34 is on an IS of 1,319 bp with a terminal repeat of seven A residues. A cluster of ORFs, ORF33 to -35, is located in reverse orientation compared to the conserved genes for structural components (described below). These facts strongly suggest that this region was transferred horizontally. The third AT island (region R3) around the right *cos* of  $\phi$ RSA1 contains only ORF51 with an unknown function.

The entire genomic comparison for these phages suggests that  $\phi$ RSA1 is closely related to *B. pseudomallei* phage  $\phi 52237$  and *P. aeruginosa* phage  $\phi$ CTX, which belong to the P2-like phages. So far, genomic sequences of a number of P2-related phages from various bacteria have been reported in the literature or in the databases, including P2 (GenBank accession no. NC001895), 186 (GenBank accession no. U32222),  $\phi 108$  (7), Fels-2 (35), HP1 (14), HP2 (41), K139 (29), and  $\phi$ Mja-PHL101 (25). Many of these phages infect bacteria belonging to the family *Enterobacteriaceae* and have the same genomic organization (with minor variations) that has been best characterized for coliphage P2 (39). The well-established P2 gene organization is compared with that of  $\phi$ RSA1 in Fig. 1 (bottom). The

FIG. 2. Matrix comparison of the genomic nucleotide sequences of  $\phi$ RSA1 and  $\phi 52237$  (A),  $\phi$ RSA1 and  $\phi$ CTX (B), and  $\phi$ RSA1 and  $\phi$ RSX (C). Nucleotide positions are shown along the genomic sequence. Fifteen matches between 20 nucleotide sequences are marked by dots (DNASIS). The base distribution along the phage genomes (percent G+C, 60-bp windows) are also shown. Regions R1 to R4 are the same as in Fig. 1.



gray shading is based on a matrix comparison of the nucleotide sequences (more than 12 matches between 15 nucleotide sequences are marked) (data not shown). As shown here, the left two-thirds of the  $\phi$ RSA1 genome that showed a high degree of homology with the  $\phi$ CTX and  $\phi$ 52237 genomes (Fig. 2B) also shared homology with phage P2, even with a difference in G+C content (50.2% in P2 DNA). This conserved region corresponds to the P2 late region, including genes for phage structural components, assembly, and regulation (6). The homology-disrupting AT islands corresponding to R1, R4, and R3, which contain four nonessential genes, *orf30*, *fun(Z)*, *tin*, and *old*, were also found in P2 (Fig. 1, bottom) (6). A region containing *lys* genes is also distinct (see below). Contrasting to the highly conserved structural modules, the right one-third of P2 DNA, containing genes for early functions and *int/att*, is remarkably different from that of  $\phi$ RSA1. Especially the locations of *int* and *att* are quite different between the two phages; they are immediately to the right of *ogr* in P2 but to the left of *cosR* in  $\phi$ RSA1 (see below). In this respect, two types of P2-like phages are obvious, P2-type and  $\phi$ RSA1-type phages, including  $\phi$ CTX and  $\phi$ 52237.  $\phi$ 108 and  $\phi$ Mja-PHL101, which infect *Pasteurella maltocida* and *Mannheimia haemolytica*, respectively (both belong to the family *Pasteurellaceae*), are also of the latter type.

It is noteworthy that the G+C content of the segment corresponding to the P2 early genes and *int/att* is slightly lower than the rest of the genome in all of these phages, even in P2 (data not shown). It might be possible that this region was derived from foreign genomes. The patchy genetic relationship between  $\phi$ RSA1 and these phages indicates frequent recombinations within the  $\phi$ RSA1 ancestral genome during its evolution, as suggested for tailed phages and their prophages (8, 9, 22).

**Genes for capsid synthesis and DNA packaging.**  $\phi$ RSA1 possesses homologues of almost all of the P2 genes required for capsid synthesis and DNA packaging in the left end of the genome in the same order as in P2 (Table 2 and Fig. 1). ORF5 and ORF6 correspond to homologues of the portal protein, gpQ, and the large subunit of terminase, gpP, respectively. *orf6* and *orf5* are adjacent in the same direction as in the PQ operon of P2, suggesting a single transcription unit. *orf7*, *-8*, *-9*, and *-10* encode homologues of the scaffold protein, gpO; the major capsid protein, gpN; the small subunit of terminase, gpM; and the head completion protein, gpL, respectively, in the same order as in P2. An icosahedral morphology and dimension of the  $\phi$ RSA1 head resembling the P2 head reflect the high homology seen in the amino acid sequences and sizes of these capsid proteins, for example, 50% amino acid identity between the ORF7 and P2 gpO proteins and 56% amino acid identity between the ORF8 and P2 gpN proteins. As described below, the DNA sequence of the  $\phi$ RSA1 *cos* site is similar to those of the P2-like phages, according to the high homology seen in the amino acid sequence and size between ORF6 and ORF9 and P2 gpP and gpM, respectively (59% amino acid identity between ORF6 and P2 gpP and 45% identity between ORF9 and P2 gpM).

**Genes for tail synthesis.** One characteristic feature of  $\phi$ RSA1 particles is their unusual tail and tail sheath structure. As shown in Fig. 3, a tail  $110 \pm 8$  nm in length and  $3 \pm 0.2$  nm in diameter is associated with a tail sheath ( $40 \pm 6$  nm in length

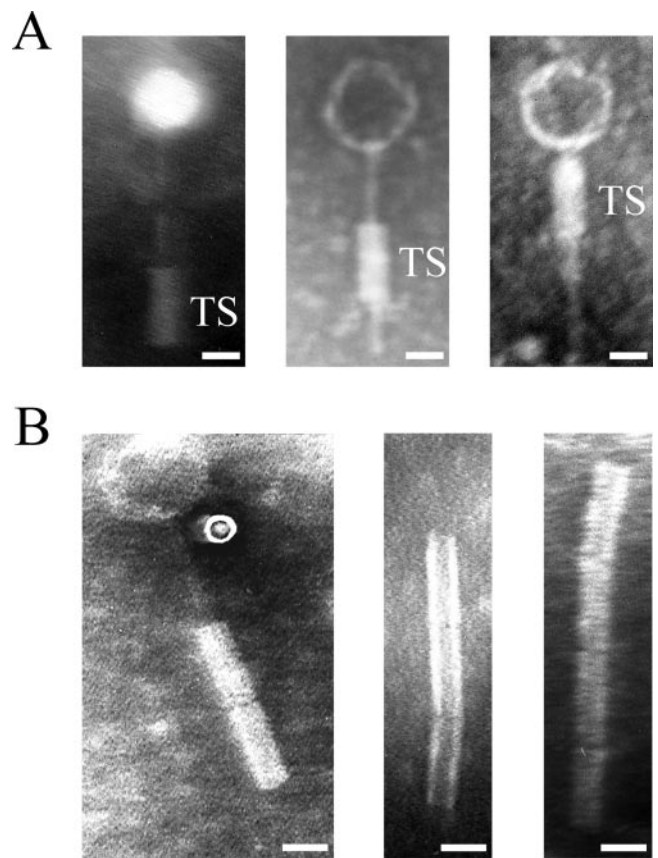


FIG. 3. Electron micrographs showing morphology of  $\phi$ RSA1 particles. A tail sheath (TS) with a constant size (40 nm in length) moves along the thin tail structure (A). Sometimes structures resembling the tail sheath are connected in a chain (B). Bars, 20 nm.

and  $17 \pm 1.5$  nm in diameter) movable along the tail (Fig. 3A). A tail sheath was often observed attached at the bottom of the tail but sometimes at intermediate positions along the tail, giving unique structures which resemble the morphology reported for *B. cepacia* phage KS5 (46). One possibility is that after attachment to the host cells the sheath contracts or moves up along the tail to bring the tail tube into the surface of the cell. Tail fibers and collar structures were not discerned from the electron micrographs (52). Sometimes, structures resembling the tail sheath were observed connected in a chain (Fig. 3B).

$\phi$ RSA1 also possesses homologues of most P2 tail genes in a gene arrangement similar to that of P2. In P2, a total of 16 essential genes were identified arranged within three operons for the tail assembly (16, 17).  $\phi$ RSA1 ORF11, corresponding to P2 gpX (with 60% amino acid identity), is located next to ORF10 (gpL homologue) at the junction of the head gene cluster and the tail and lysis gene cluster. ORF16 and ORF17 (corresponding to P2 tail completion proteins gpR and gpS, respectively) are found after the lysis genes. Moderate amino acid identity was observed between these genes (46% amino acid identity between ORF16 and P2 gpR and 40% identity between ORF17 and P2 gpS). The second gene cluster for tail assembly comprised seven ORFs (ORF19 to ORF25). ORF19 to -21 are homologues of the P2 baseplate assembly proteins



gpV (41% amino acid identity), gpW (39% amino acid identity), and gpJ (62% amino acid identity), respectively. ORF22 showed homology to P2 tail formation protein gpI (52% amino acid identity). ORF23 is a homologue of P2 tail fiber protein gpH, and ORF24 is a C-terminal portion of ORF23, which is described as a putative tail fiber protein (RSc1692; accession no. Q8XYR6). Although the 150-amino-acid N-terminal portion of ORF23 showed high amino acid identity (54%) with P2 gpH, the remaining part showed only marginal homology. The C-terminal part of P2 gpH is made up of several modules that are found in the tail fiber proteins of a variety of double-stranded DNA phages in various combinations (16). ORF25 is located at a position corresponding to that of P2 tail fiber assembly protein gpG, but its size, 250 amino acids (aa), is larger than that of gpG (175 aa) and the amino acid identity is low, only 25%. This is also the case in  $\phi$ CTX; there was no  $\phi$ CTX ORF with significant homology to P2 gpG;  $\phi$ CTX ORF21 seemed to have replaced it (38). In contrast to the highly conservative nature of other structural proteins in P2-like phages, this tail fiber assembly protein may be highly specific to each phage.

Another gene cluster for tail formation includes six ORFs (ORF27 to -32) corresponding to the P2 gene cluster *gpFI-gpFII-gpE-gpT-gpU-gpD*. High amino acid identity was observed between ORF27 and P2 major tail sheath protein gpFI (62% identity) and between ORF28 and P2 tail tube protein gpFII (47% identity), but all other homologues shared moderate homologies ranging from 35% to 44% amino acid identity. As described above, the  $\phi$ RSA1 particles showed characteristic tail structures somewhat different from those of P2 and typical P2-related phages, which reflects the differences observed in ORFs included in these tail assembly structural modules.

**Lysis genes.**  $\phi$ RSA1 encodes four ORFs (*orf12* to *orf15*) in the region corresponding to the P2 region for lysis function, where five genes (*gpY*, *gpK*, *lysA*, *lysB*, and *lysC*) are located. *orf12* and *orf13* encode highly hydrophobic small (possibly transmembrane) proteins related to holins which form the channels in the cytoplasmic membranes for the translocation of lytic enzymes (53), although no significant amino acid sequence identity was detected between these ORFs and P2 holin gpY.  $\phi$ RSA1 ORF14 showed high amino acid sequence homology with various phage lytic enzymes (unpublished data). ORF14 exhibited an amino acid sequence almost identical to that of an ORF (RSc1931) detected on the chromosome of *R. solanacearum* GMI1000 (98% identity), and an amino acid identity as high as 57% with lytic enzymes of  $\phi$ 52237 and  $\phi$ CTX was observed. A composite structure of the  $\phi$ CTX lytic enzyme consisting of the N-terminal region conserved in the gram-positive bacteria and their phages and the C-terminal region shared by lytic enzymes of lipid-containing phages was reported (38). The high observed homology with these enzymes suggests that the  $\phi$ RSA1 ORF14 protein may function in cells of *P. aeruginosa* and *B. pseudomallei* as well. In contrast to this, P2 endolysin gpK (166 aa) did not show significant amino acid sequence homology to these enzymes. Homologues of P2 *lysA* (which affects the timing of lysis), *lysB* (for the regulation of lysis), and *lysC* (a transcription attenuator) are not clear in  $\phi$ RSA1, although ORF14 showed marginal

homology with both P2 *lysA* (30% amino acid identity) and *lysB* (30% identity).

**Regulatory genes for late gene expression and possible late promoters.** The expression of the P2-related phage late genes is absolutely dependent on the Ogr proteins (4, 10). The Ogr protein family represents a unique group of prokaryotic zinc finger DNA-binding transcriptional activators which are highly conserved in P2-related phages. A set of four cysteine residues is conserved in all Ogr proteins in the arrangement C-(X)<sub>2</sub>-C-(X)<sub>22</sub>-C-(X)<sub>4</sub>-C, where a zinc ion is coordinated by four cysteines (32). The Ogr protein interacts with the  $\alpha$  subunit of RNA polymerase and activates the late-gene promoters (3, 31). On the P2 genome, the *ogr* gene is located immediately downstream of the gene cluster *gpF-gpE-gpT-gpU-gpD* close to *attP* and the *int* gene (11). A possible *ogr* homologue,  $\phi$ RSA1 *orf38*, that has 34% amino acid identity with P2 Ogr and contains precisely the conserved zinc finger motif, was found approximately 3.4 kb downstream from the *gpD* homologue (*orf32*) on the  $\phi$ RSA1 genome (Table 2 and Fig. 1). As described above, this is caused by an insertion of a 3.4-kb region (region R2) with five ORFs, including ISRSO15.

The consensus binding sequence for Ogr proteins has been identified in each late promoter region in the P2 family as TGT-(N)<sub>12</sub>-ACA, which is central approximately at the -55 position from the first ATG codon (28). In  $\phi$ RSA1, four possible late promoter regions (5' noncoding regions of *orf6*, *orf7*, *orf19*, and *orf27*) were examined for such sequence motifs or common sequences. All of these regions contained a sequence motif [5' TGTTGT-(X)<sub>13</sub>-ACAACA] that is centered around positions -50 to -89 from the initiation codon (unpublished data). This sequence is related to the P2 consensus sequence, indicating that  $\phi$ RSA1 Ogr may have the same promoter recognition mechanism as the Ogr proteins of the P2 family. No promoter sequence of the  $\sigma^{70}$  type was present in these possible late promoter regions of  $\phi$ RSA1.

**Early genes and genes for lysogeny.** On the right side of ORF38 (Ogr homologue), there are 12 ORFs (ORF39 to -51) arranged in the same direction and 1 ORF (ORF48) that overlaps ORF47 in the reverse orientation. Because both ORF47 and -48 showed homologous sequences in the databases, they are included in Table 2 and Fig. 1. In P2, this genomic region contains early-expressed genes, including genes for DNA replication (34) such as *gpA* and *gpB*, genes for lysogeny such as the integrase gene and *cox* (43), and genes for lysogenic conversion such as *old* (37) and *tin* (36). These  $\phi$ RSA1 ORFs did not show significant similarity to the P2 genes in the corresponding region, whereas their homologous sequences were found in the databases for various phages or prophages, especially of *Ralstonia* species and *Burkholderia* species. For example, ORF39 showed 65% amino acid identity with *B. pseudomallei* phage  $\phi$ 52237 ORF15 (accession no. AAZ72616.1), 65% identity with the prophage sequence in *B. pseudomallei* strain K96243 (accession no. Q63YQ0), and 41% identity with the prophage antirepressor sequence of *Xylella fastidiosa* strain Ann-1 (accession no. Q3R0Y7).  $\phi$ RSA1 ORF47 (the largest ORF of  $\phi$ RSA1) showed 74% amino acid identity with  $\phi$ 52237 ORF4 (accession no. AAZ72605.1), 74% identity with the prophage sequence of *B. pseudomallei* strain K96243 (accession no. Q63YQ8), 51% identity with the *R. solanacearum* NCBI305 prophage sequence RSc0967 (acces-

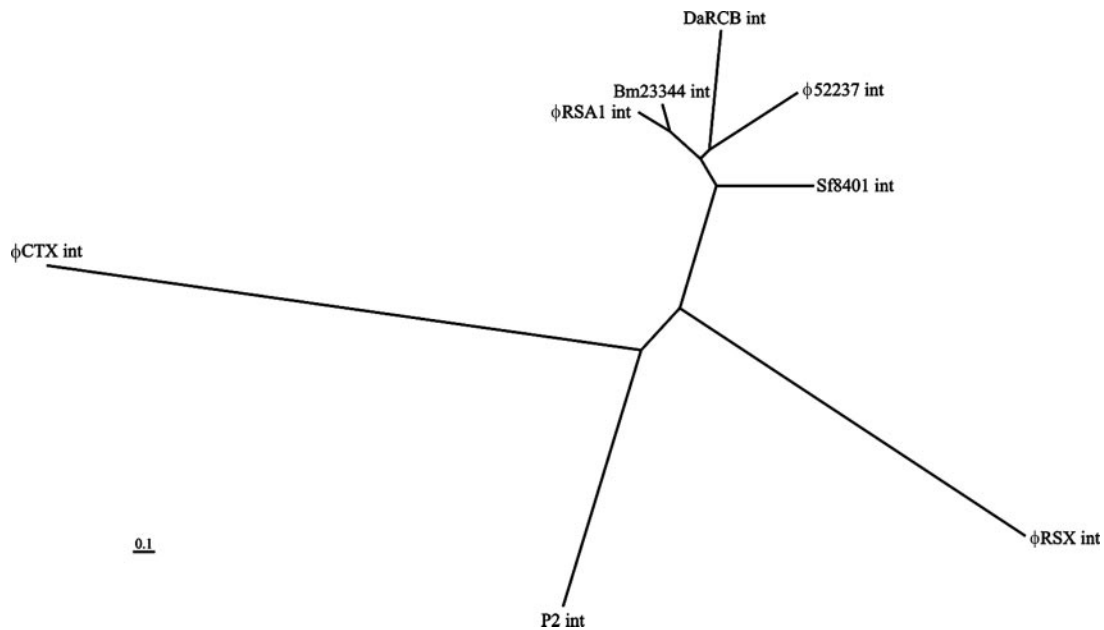


FIG. 4. Phylogenetic tree based on the alignment phage *int* ORFs. The amino acid sequence of  $\phi$ RSA1 ORF50 is compared with *int* sequences of Bm23344 (accession no. Q62FM0),  $\phi$ 52237 (accession no. Q45Y16), DaRCB (accession no. Q47H88), Sf8401 (accession no. Q0T7U1), P2 (accession no. P36932),  $\phi$ RSX (accession no. Q8Y3C8), and  $\phi$ CTX (accession no. Q38644). The analysis was performed by the multiple-alignment program CLUSTAL W.

sion no. Q8Y0S6), and 51% identity with the prophage sequence of *R. eutropha* JMP134 (accession no. Q46Z72). Although the function of this well-conserved ORF is not known, a 150-amino-acid portion at the N terminus showed 42% amino acid identity with some bacterial DNA primases (accession no. Q43KY5), suggesting its involvement in DNA replication.  $\phi$ RSA1 ORF50 is a homologue of *int* of the P2-related phages (unpublished data). Its amino acid sequence shows various degrees of homology to *int* sequences of P2-related phages and prophages. Based on the sequence alignment data, a phylogenetic tree was constructed as shown in Fig. 4, which suggests a close relatedness of integrases of  $\phi$ RSA1 and the prophage integrated in the chromosome of *B. mallei* ATCC 23344 (accession no. Q62FM0).

To verify the possible functions for DNA replication of ORFs in this region,  $\phi$ RSA1 minireplicons were constructed. A P2 minireplicon was constructed with a small region containing gene *A* and *ori* (34). However, as suggested by the genome comparison in Fig. 1 (bottom), the gene organization required for DNA replication may be different in  $\phi$ RSA1. In fact, such a minireplicon could not be obtained for  $\phi$ CTX (38), and to our knowledge, no successful example has been reported from " $\phi$ RSA1-type" phages so far.  $\phi$ RSA1 DNA fragments containing ORF49 and its upstream ORFs were amplified by PCR with a combination of primers as shown in Table 1 and Fig. 1. Three fragments of 10.4 kbp (amplified with primers ORF33-P1 and ORF49-P4), 7.7 kbp (amplified with primers ORF36-P2 and ORF49-P4), and 6.7 kbp (amplified with primers ORF39-P3 and ORF49-P4), as indicated in Fig. 1 (fragments A, B, and C, respectively), were connected to a  $Km^r$  cassette of 1.5 kbp and introduced into cells of *R. solanacearum* strains M4S and MAFF106611 by electroporation. The resulting minireplicon of 11.5 kbp was stably maintained in the cells

and conferred  $Km^r$  on the cells, indicating that *ori* and functions necessary for  $\phi$ RSA1 DNA replication are encoded within this region. However, neither the 7.7-kbp nor the 6.7-kbp  $\phi$ RSA1 fragment could support stable replication of the DNA constructs. Some ORFs (ORF33, ORF34, and ORF35) in the 10.4-kbp fragments may be involved in plasmid maintenance. In this context, it is interesting that ORF35 resembles the DNA-binding repressor proteins of bacteriophages (Table 2). The actual involvement of ORF35 in the maintenance of the  $\phi$ RSA1 minireplicon was confirmed by removing a 2.0-kbp fragment containing ORF33 and ORF34 from the 10.4-kbp construct by PCR with primers ORF35-P5 and ORF49-P4 (Table 1). The resulting construct of 8.2 kbp (D in Fig. 1, top) was stably maintained in cells of both strains M4S and MAFF 106611 on selection plates containing kanamycin.  $\phi$ RSA1 ORF35 showed amino acid sequence similarity to  $\phi$ RSX RSc1907 (E value of  $7e-20$ ) and  $\phi$ 52237 gp23 (Q63YP6; E value of  $6e-21$ ). This is the first successful example of a minireplicon of  $\phi$ RSA1-type phages.

**$\phi$ RSA1 *cos* and *att* sequences.** On pulsed-field gel electrophoresis, the  $\phi$ RSA1 DNA showed a ladder pattern with a monomer size of approximately 39 kb, like coliphage  $\lambda$  (52), suggesting the presence of cohesive ends (*cos*) on the linear molecule. When  $\phi$ RSA1 DNA was digested with HincII, more than 20 fragments were generated, among which was a 5.7-kb fragment that dissociated into two fragments (2.4 and 3.3 kb) after heating at 70°C for 15 min. The 5.7-kb HincII fragment extracted from agarose gel after electrophoresis was heated to generate the two bands, which were treated with T4 DNA polymerase to form blunt ends. After connecting to the EcoRV site of pBluescript II SK+, the fragments were cloned and sequenced. By comparing the nucleotide sequences to each other and with the  $\phi$ RSA1 genomic sequence, it was revealed

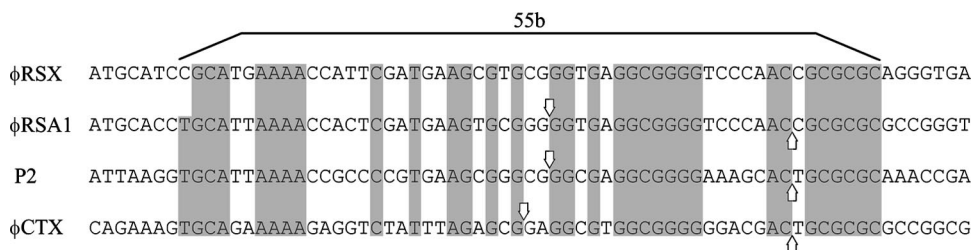


FIG. 5. Comparison of the *cos* region of ϕRSA1 with those of P2-related phages. Bases within the 55-bp core sequence that are shared by phages (54) are shaded. Downward and upward vertical arrows indicate *cos* cleavage sites. The exact cohesive end of ϕRSX is unknown.

that a 19-base sequence of the 3' end of the 2.4-kb fragment is the same as a 19-base sequence of the 5' end of the 3.3-kb fragment, indicating that the ϕRSA1 DNA contains a 19-base single-stranded extrusions on the left (5'-GGTGAGGCGGG GTCCCAAC-3') and on the right (3'-CCACTCCGCCCCAG GTTG-5'). In Fig. 5, the ϕRSA1 *cos* sequence is compared with those of a few phages of the P2 family, including P2 and ϕCTX. A 55-bp core sequence (54) was also found to be well conserved in ϕRSA1. Both ϕRSA1 and P2 have 19-base 5'-extruding cohesive ends, but ϕCTX has a 21-base 5' extrusion (19).

ϕRSA1 was spontaneously released from *R. solanacearum* strain MAFF211272, and a ϕRSA1-related sequence was detected on the chromosomal DNA of this strain, indicating that ϕRSA1 contains an attachment site (*attP*) where it recombines with a homologous sequence on the bacterial genome (*attB*) via site-specific recombination (12). As described above, ϕRSA1 encodes a site-specific integrase (ORF50, *int*), and an *attP* sequence was predicted in the vicinity of this gene, as seen in most P2-related phages. Chromosomal DNA fragments of strain MAFF211272 that contain flanking regions of the ϕRSA1 prophage were cloned as follows. Two *HincII* fragments (2.6 and 6.0 kb), which showed different patterns compared with *HincII* fragments in Southern blot hybridization, were extracted from the agarose gel, connected to pBluescript II SK+, and cloned into *E. coli* XL10 Gold. The nucleotide sequence of the 2.6-kb fragment contained a ϕRSA1 sequence region containing ORF50 (*int*), followed by 88 bases overlapping the gene for arginine tRNA(CCG), after which a chromosomal sequence appeared. On the 6.0-kb fragment, a chromosomal sequence was connected to a ϕRSA1 sequence corresponding to a 45-base 3' portion of the arginine tRNA(CCG) gene, followed by ORF51. These results demonstrated that ϕRSA1 used a 45-base 3' portion of the arginine tRNA(CCG) gene as *attP* and was integrated into the arginine tRNA(CCG) gene on the chromosome of strain MAFF211272 as indicated in Fig. 6. It is also interesting that ϕRSA1 *att* sequence was present in the chromosomal DNA of *B. pseudomallei* strain 1026b (accession no. AY471582), indicating that a ϕRSA1-related phage may also infect this bacterial species and integrate at the same *att* site. For comparison, we examined the nucleotide sequence of *B. pseudomallei* phage ϕ52237 for a possible *att* sequence and found in the corresponding region (positions 2845 to 2889, accession no. DQ087285) a 45-base 3' portion of the phenylalanine tRNA-(GAA) gene. Therefore, ϕRSA1 and ϕ52237 use different tRNA genes as an *att* site. P2-like phages and their satellite

phages 186, P4, Hp1, R73, and ϕCTX use tRNA genes as *attB* as well (18, 19, 33, 40, 48).

**Other genes.** In addition to unknown genes located in the AT islands, such as *orf18*, *orf36*, *orf37*, and *orf51* as described above, ϕRSA1 contained four additional ORFs (ORF1 to ORF4) between *cosL* and ORF5 (P2 gpQ homologue), as shown in Table 2 and Fig. 1. Interestingly this position is also suggested as another hot spot on the P2-like phage genomes where foreign genes can be picked up without disturbing the functions of other genes (13, 38). ϕRSA1 ORF1, -2, and -4 show some amino acid sequence similarity to proteins of *Janthinobacterium lividum*, and ORF3 is similar to a hypothetical protein (accession no. Q2SWS5) of *B. thailandensis*. These genes might have been acquired from previous hosts, suggesting a wide host range of ϕRSA1 extending to *Burkholderia-Janthinobacterium* species.

**Homology to the prophage sequence detected on the *R. solanacearum* GMI1000 chromosome.** On the 3.7-Mb chromosome of *R. solanacearum* GMI1000, at least four possible prophage sequences were detected (44). One of them, a 40.7-kb region located at positions 2,084,442 to 2,125,154 (designated ϕRSX), showed significant nucleotide similarity to ϕRSA1. This prophage sequence was briefly described as RS6 previously (9). Figure 2C shows a matrix comparison of the nucleotide sequences of the ϕRSA1 genome and the ϕRSX chromosomal region. As shown in the comparison of ϕRSA1 and ϕCTX (Fig. 2B), the two-thirds portion of the left side of the ϕRSA1 genome that encodes the structural modules showed a high level of homology to the ϕRSX sequence and the homology is interrupted by the AT island R2 as described above. Therefore, the possible prophage ϕRSX can also be a member of the family of P2-like phages and retains conserved structural modules, even with a somewhat larger entire-genome size. This is supported by additional information as follows. In the ϕRSX region, there is a gene for serine tRNA(GGA) at positions 2,084,367 to 2,084,457 immediately upstream of the possible integrase ORF (RSc1896). A 15-bp sequence at the 3' end of this gene was found to be repeated at positions 2,125,140 to 2,125,154, which separates the phage-related sequences from the chromosomal sequences, suggesting that the sequence of serine tRNA(GGA) is *attL* and the 15-bp sequence at the 3' end of this gene is *attR* on the chromosome of strain GMI1000, as depicted in Fig. 6B. In the vicinity of this *attR* region, there is a sequence closely related to *cos* at positions 2,121,802 to 2,121,858. This possible *cos* sequence of ϕRSX is compared with those of other phages in



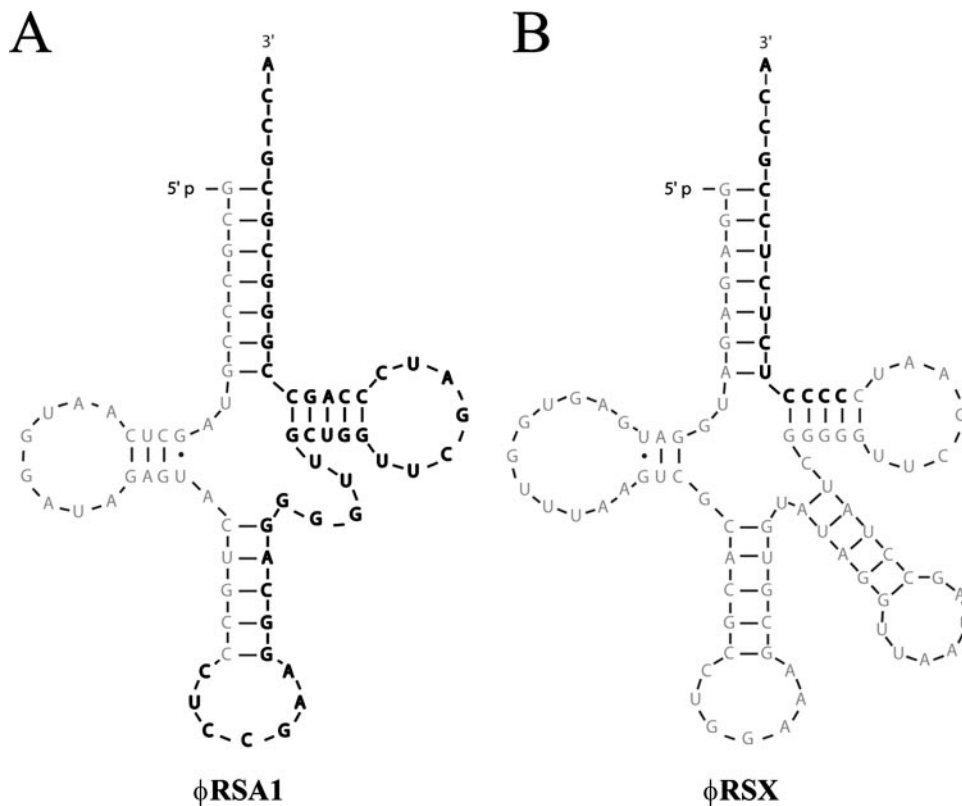


FIG. 6. *attP* sequences of  $\phi$ RSA1 and  $\phi$ RSX. The  $\phi$ RSA1 and  $\phi$ RSX attachment sites correspond to a 45-base 3' portion of the arginine tRNA(CCG) (A) and a 15-base 3' portion of the serine tRNA(GGA) (B), respectively. The *attP* core nucleotide sequence is in bold letters.

Fig. 5. As shown here, only five nucleotides of the conserved 55 bp are different between  $\phi$ RSA1 and  $\phi$ RSX.

All of the  $\phi$ RSA1 ORFs for the P2-like phage structural proteins identified (Table 2) are also highly conserved in  $\phi$ RSX (compared with  $\phi$ RSA1 in Fig. 1, bottom). In the database search for homology to these  $\phi$ RSA1 proteins, the highest BLAST scores were always obtained with  $\phi$ RSX proteins (RSc1899 to RSc1941), as indicated in Table 2; in each comparison of the  $\phi$ RSA1 and  $\phi$ RSX counterparts, amino acid identity ranged from 85% (gpX;  $\phi$ RSA1 ORF11 versus  $\phi$ RSX RSc1934) to 100% (gpS;  $\phi$ RSA1 ORF17 versus  $\phi$ RSX RSc1928), indicating a very close relatedness of  $\phi$ RSA1 and  $\phi$ RSX. In contrast to this high degree of similarity in the organization of structural genes, RSA1 regions R1, R2, and R3 also interrupted the sequence homology between  $\phi$ RSA1 and  $\phi$ RSX (Fig. 2C). In the  $\phi$ RSX sequence (67.0% average G+C content), region R1 corresponds to an ACUR of 1,512 bp (51.5% G+C) containing RSc1926 and RSc1927 (without known functions), and  $\phi$ RSX region R2 coincided with another ACUR of 2,657 bp (56.7% G+C) containing six ORFs (RSc1905, RSc1906, RSc1907, RSc1908, RSc1909, and RSc1910). Among them, only RSc1907 showed a relatively low amino acid sequence similarity to  $\phi$ RSA1 ORF35 (39% identity). RSc1907 is noted as a putative phage DNA-binding repressor (accession no. Q8XY56). Within the  $\phi$ RSX-R2 region, there is no IS (ISRSO15) that was observed in the corresponding region of the  $\phi$ RSA1 sequence. The  $\phi$ RSX sequence corresponding to region R3 overlaps another ACUR of 3,427 bp

(56.5% G+C) containing two unknown ORFs (RSc1947 and RSc1948). The  $\phi$ RSX ORFs around this region, including RSc1896 (*int*), RSc1897, RSc1898, RSc1945, and RSc1946, did not show significant homology to  $\phi$ RSA1 ORFs in the corresponding positions. For example, the amino acid identity between  $\phi$ RSA1 ORF50 (*int*) and RSc1896 (*int*) is only 29% (unpublished data).

In addition to these nonconserved regions, a region between *cosL* and *gpQ* is also divergent between  $\phi$ RSA1 and  $\phi$ RSX. There is a *vgr*-like gene (RSc1944) located close to *cos* of  $\phi$ RSX. Wang et al. (49) considered the *vgr* gene a structural component of at least some *Rhs* (recombination hot spot) elements. The functions of two other ORFs (RSc1942 and RSc1943) located in this  $\phi$ RSX region are not known. There is a long repeat sequence within the coding region of RSc1942.

These nonconserved regions may have been rearranged very recently, possibly by horizontal gene transfers in the divergence of  $\phi$ RSA1 and  $\phi$ RSX. In the light of the gene arrangement found in P2-like phage  $\phi$ RSA1, the prophage  $\phi$ RSX sequence was characterized in this work.

**Prophage effects of  $\phi$ RSA1 on lysogenic cells.** Some temperate phages and prophages are known to carry additional cargo genes (termed morons or lysogenic conversion genes). Many morons from prophages in pathogenic bacteria encode proven or suspected virulence factors (5, 8, 23, 27). The cytotoxin gene (*ctx*) was found to be inserted at an AT island in  $\phi$ CTX of *P. aeruginosa* (38). The *ctx* gene appeared to have jumped in between *cos* and *orfI* (*gpQ* equivalent) (Fig. 1, top),

suggesting that this region is a hot spot for such genes. Within this corresponding region of  $\phi$ RSA1, there are four ORFs (ORF1 to ORF4) in the same orientation as described above. In the  $\phi$ RSX sequence, integrated in *R. solanacearum* GMI1000, three ORFs, RSc1944, RSc1943, and RSc1942, are also found in the same orientation as described above and comapped in Fig. 1, bottom. Compared to cells without  $\phi$ RSA1 sequences, the lysogenic cells showed no obvious changes in growth rate, cell morphology, colony morphology, pigmentation, or extracellular polysaccharide production in culture. In our preliminary infection experiments, no obvious enhanced pathogenicity was observed with  $\phi$ RSA1 lysogenic cells by in planta virulence assay with tobacco plants. However, these extra genes are still interesting subjects for further analyses concerning pathogenesis-related physiological functions.

**Conclusion.** (i) A bacteriophage,  $\phi$ RSA1, with an especially wide host range of *R. solanacearum* has been characterized as a P2-related phage by genomic analysis. With the established gene organization, this phage might be useful as a biocontrol agent or a biodiagnosis tool for bacterial wilt disease. (ii) One putative prophage sequence (previously named RS6 [9]) detected on the chromosome of *R. solanacearum* strain GMI1000 has been characterized in detail as a  $\phi$ RSA1-related prophage (designated  $\phi$ RSX in this work). Extra genes found in the hot-spot regions of these phage genomes may be candidates for further studies related to the pathogenesis of this wilt disease bacterium. (iii) A stable minireplicon has been constructed from an 8.2-kbp early region of  $\phi$ RSA1 DNA. This is the first example of a minireplicon from  $\phi$ RSA1-type phages and will serve as a good system to study the unknown replication mechanism of related phages.

#### ACKNOWLEDGMENTS

We are grateful to W. C. Nierman for allowing us to use his  $\phi$ 52237 sequence data in comparative analyses prior to their publication.

This study was supported by the Industrial Technology Research Grant Program in 04A09505 from the New Energy and Industrial Technology Development Organization (NEDO) of Japan.

#### REFERENCES

- Altschul, S. F., T. L. Madden, A. A. Schaffer, Z. Zhang, W. Miller, and D. J. Lipman. 1997. Gapped BLAST and PSI-BLAST: a new generation of protein database search programs. *Nucleic Acids Res.* **25**:3389–3402.
- Ausubel, F., R. Brent, R. E. Kingston, D. D. Moore, J. G. Seidman, J. A. Smith, and K. Struhl. 1995. Short protocols in molecular biology, 3rd ed. John Wiley & Sons, Inc., Hoboken, NJ.
- Ayers, D. J., M. G. Sunshine, E. W. Six, and G. E. Christie. 1994. Mutations affecting two adjacent amino acid residues in the alpha subunit of RNA polymerase block transcriptional activation by the bacteriophage P2 Ogr protein. *J. Bacteriol.* **176**:7430–7438.
- Birkeland, N. K., G. E. Christie, and B. H. Lindqvist. 1988. Directed mutagenesis of the bacteriophage P2 *ogr* gene defines an essential function. *Gene* **73**:327–335.
- Brüssow, H., C. Canchaya, and W.-D. Hardt. 2004. Phages and the evolution of bacterial pathogens: from genomic rearrangements to lysogenic conversion. *Microbiol. Mol. Biol. Rev.* **68**:560–602.
- Calendar, R., S. Yu, H. Myung, V. Barreiro, R. Odegrip, K. Carlson, L. Davenport, G. Mosig, G. E. Christie, and E. Haggård-Ljungquist. 1998. The lysogenic conversion genes of coliphage P2 have unusually high AT content, p. 241–252. *In* M. Syvanen and C. Kado (ed.), *Horizontal gene transfer*. Chapman & Hall, Ltd., London, United Kingdom.
- Campoy, S., J. Aranda, G. Alvarez, J. Barbe, and M. Llagostera. 2006. Isolation and sequencing of a temperate transducing phage for *Pasteurella multocida*. *Appl. Environ. Microbiol.* **72**:3154–3160.
- Canchaya, C., C. Proux, G. Fournous, A. Bruttin, and H. Brussow. 2003. Prophage genomics. *Microbiol. Mol. Biol. Rev.* **67**:238–276.
- Casjens, S. 2003. Prophages and bacterial genomics: what have we learned so far? *Mol. Microbiol.* **49**:277–300.
- Christie, G. E., E. Haggård-Ljungquist, R. Feiwell, and R. Calendar. 1986. Regulation of bacteriophage P2 late gene expression: the *ogr* gene. *Proc. Natl. Acad. Sci. USA* **83**:3238–3242.
- Christie, G. E., L. M. Temple, B. A. Bartlett, and T. S. Goodwin. 2002. Programmed translational frameshift in the bacteriophage P2 FETUD tail gene operon. *J. Bacteriol.* **184**:6522–6531.
- Craig, N. L. 1988. The mechanism of conservative site-specific recombination. *Annu. Rev. Genet.* **22**:77–105.
- Dodd, I. B., and J. B. Egan. 1996. The *Escherichia coli* retrons Ec67 and Ec86 replace DNA between the *cos* site and a transcription terminator of a 186-related prophage. *Virology* **219**:115–124.
- Esposito, D., W. P. Fitzmaurice, R. C. Benjamin, S. D. Goodman, A. S. Waldman, and J. J. Scocca. 1996. The complete nucleotide sequence of bacteriophage HP1 DNA. *Nucleic Acids Res.* **24**:2360–2368.
- Gatt, R., and E. R. Berman. 1966. A rapid procedure for the estimation of amino sugars on a microscale. *Anal. Biochem.* **15**:167–171.
- Haggård-Ljungquist, E., C. Halling, and R. Calendar. 1992. DNA sequences of the tail fiber genes of bacteriophage P2: evidence for horizontal transfer of tail fiber genes among unrelated bacteriophages. *J. Bacteriol.* **174**:1462–1477.
- Haggård-Ljungquist, E., K. Jacobsen, S. Rishovd, W. Six, O. Nilssen, M. G. Sunshine, B. H. Lindqvist, K.-J. Kim, V. Barreiro, E. V. Koonin, and R. Calendar. 1995. Bacteriophage P2: genes involved in baseplate assembly. *Virology* **213**:109–121.
- Hauser, M. A., and J. J. Scocca. 1990. Location of the host attachment site for phage HP1 within a cluster of *Haemophilus influenzae* tRNA genes. *Nucleic Acids Res.* **18**:5305.
- Hayashi, T., H. Matsumoto, M. Ohnishi, and Y. Terawaki. 1993. Molecular analysis of a cytotoxin-converting phage,  $\phi$ CTX, of *Pseudomonas aeruginosa*: structure of the *attP-cos-ctx* region and integration into the serine tRNA gene. *Mol. Microbiol.* **7**:657–667.
- Hayward, A. C. 1991. Biology and epidemiology of bacterial wilt caused by *Pseudomonas solanacearum*. *Annu. Rev. Phytopathol.* **29**:65–87.
- Hayward, A. C. 2000. *Ralstonia solanacearum*, p. 32–42. *In* J. Lederberg (ed.) *Encyclopedia of microbiology*, vol. 4. Academic Press, San Diego, CA.
- Hendrix, R. W., G. F. Hatfull, and M. C. M. Smith. 2003. Bacteriophages with tails: chasing their origins and evolution. *Res. Microbiol.* **154**:253–257.
- Hendrix, R. W., J. G. Lawrence, G. F. Hatfull, and S. Casjens. 2000. The origins and ongoing evolution of viruses. *Trends Microbiol.* **8**:504–508.
- Higashiyama, T., and T. Yamada. 1991. Electrophoretic karyotyping and chromosomal gene mapping of *Chlorella*. *Nucleic Acids Res.* **19**:6191–6195.
- Highlander, S. K., S. Weissenberger, L. E. Alvarez, G. M. Weinstock, and P. B. Berget. 2006. Complete nucleotide sequence of a P2 family lysogenic bacteriophage,  $\phi$ MhaA1-PHL101, from *Mannheimia haemolytica* serotype A1. *Virology* **350**:79–89.
- Horita, M., and K. Tsuchiya. 2002. MAFF microorganism genetic resources manual no. 12, p. 5–8. National Institute of Agricultural Sciences, Tsukuba, Japan.
- Juhala, R. J., M. E. Ford, R. L. Duda, A. Youlton, G. F. Hatfull, and R. W. Hendrix. 2000. Genomic sequences of bacteriophages HK97 and HK022: pervasive genetic mosaicism in the lambdoid bacteriophages. *J. Mol. Biol.* **299**:27–51.
- Julien, B., and R. Calendar. 1995. Purification and characterization of the bacteriophage P4  $\delta$  protein. *J. Bacteriol.* **177**:3743–3751.
- Kapfhammer, D., J. Blass, S. Evers, and J. Reidl. 2002. *Vibrio cholerae* phage K139: complete sequence and comparative genomics of related phages. *J. Bacteriol.* **184**:6592–6601.
- Kawasaki, T., S. Nagata, A. Fujiwara, H. Satsuma, M. Fujie, S. Usami, and T. Yamada. 2007. Genomic characterization of the filamentous integrative bacteriophages  $\phi$ RSS1 and  $\phi$ RSM1, which infect *Ralstonia solanacearum*. *J. Bacteriol.* **189**:5792–5802.
- King, R. A., D. L. Anders, and G. E. Christie. 1992. Site-directed mutagenesis of an amino acid residue in bacteriophage P2 Ogr protein implicated in interaction with *Escherichia coli* RNA polymerase. *Mol. Microbiol.* **6**:3313–3320.
- Lee, T.-C., and G. E. Christie. 1990. Purification and properties of the bacteriophage P2 *ogr* gene product. A prokaryotic zinc-binding transcriptional activator. *J. Biol. Chem.* **265**:7472–7477.
- Lindqvist, B. H., G. Deho, and R. Calendar. 1993. Mechanisms of genome propagation and helper exploitation by satellite phage P4. *Microbiol. Rev.* **57**:683–702.
- Liu, Y., S. Saha, and E. Haggård-Ljungquist. 1993. Studies of bacteriophage P2 DNA replication. The DNA sequence of the *cis*-acting gene *A* and ori region and construction of a P2 mini-chromosome. *J. Mol. Biol.* **231**:361–374.
- Miold, S., and W.-D. Hardt. 2003. The SopE $\phi$  phage integrates into the *ssrA* gene of *Salmonella enterica* serovar Typhimurium A36 and is closely related to the Fels-2 prophage. *J. Bacteriol.* **185**:5182–5191.
- Mosig, G., S. Yu, H. Myung, E. Haggård-Ljungquist, L. Davenport, K. Carlson, and R. A. Calendar. 1997. A novel mechanism of virus-virus interactions: bacteriophage P2 Tin protein inhibits phage T4 DNA synthesis by

- poisoning the T4 single-stranded DNA binding protein gp32. *Virology* **230**:72–81.
37. Myung, H., and R. Calendar. 1995. The old exonuclease of bacteriophage P2. *J. Bacteriol.* **177**:497–501.
  38. Nakayama, K., S. Kanaya, M. Ohnishi, Y. Terawaki, and T. Hayashi. 1999. The complete nucleotide sequence of CTX, a cytotoxin-converting phage of *Pseudomonas aeruginosa*: implications for phage evolution and horizontal gene transfer via bacteriophages. *Mol. Microbiol.* **31**:399–419.
  39. Nilsson, A. S., and Haggård-Ljungquist. 2006. The P2-like bacteriophages, p. 365–390. In R. Calendar (ed.), *The bacteriophages*. ASM Press, Washington, DC.
  40. Pierson, L. S., III, and K. L. Kahn. 1987. Integration of satellite bacteriophage P4 in *Escherichia coli*. DNA sequences of the phage and host regions involved in site-specific recombination. *J. Mol. Biol.* **196**:487–496.
  41. Pontarollo, R. A., C. R. Rioux, and A. A. Potter. 1997. Cloning and characterization of bacteriophage-like DNA from *Haemophilus sommus* homologous to phage P2 and HP1. *J. Bacteriol.* **179**:1872–1879.
  42. Rosenberg, C., F. Casse-Delbart, I. Dusha, M. David, and C. Boucher. 1982. Megaplasms in the plant associated bacteria *Rhizobium meliloti* and *Pseudomonas solanacearum*. *J. Bacteriol.* **150**:402–406.
  43. Saha, S., E. Haggård-Ljungquist, and K. Nordstrom. 1989. Activation of prophage P4 by the P2 Cox protein and the site of action of the Cox protein on the two phage genomes. *Proc. Natl. Acad. Sci. USA* **86**:3973–3977.
  44. Salanoubat, M., S. Genin, F. Artiguenave, J. Gouzy, S. Mangenot, M. Ariat, A. Billault, P. Brottier, J. C. Camus, L. Cattolico, M. Chandler, N. Choisene, S. Claudel-Renard, N. Cunnac, C. Gaspin, M. Lavie, A. Molsan, C. Robert, W. Saurin, T. Schlex, P. Siguier, P. Thebault, M. Whalen, P. Wincker, M. Levy, J. Weissenbach, and C. A. Boucher. 2002. Genome sequence of the plant pathogen *Ralstonia solanacearum*. *Nature* **415**:497–502.
  45. Sambrook, J., and D. W. Russell. 2001. *Molecular cloning: a laboratory manual*, 3rd ed. Cold Spring Harbor Laboratory Press, Cold Spring Harbor, N.Y.
  46. Seed, K. D., and J. J. Dennis. 2005. Isolation and characterization of bacteriophages of *Burkholderia cepacia* complex. *FEMS Microbiol. Lett.* **251**:273–280.
  47. Smith, E. F. 1986. A bacterial disease of tomato, pepper, eggplant, and Irish potato (*Bacillus solanacearum* nov. sp.). U.S. Dept. Agric. Div. Vegetable Physiol. Pathol. Bull. **12**:1–28.
  48. Sun, J., M. Inouye, and S. Inouye. 1991. Association of a retroelement with a P4-like cryptic prophage (retrophage  $\phi$ R73) integrated into the selenocystyl tRNA gene of *Escherichia coli*. *J. Bacteriol.* **173**:4171–4181.
  49. Wang, Y.-D., S. Zhao, and C. W. Hill. 1998. *Rhs* elements comprise three subfamilies which diverged prior to acquisition by *Escherichia coli*. *J. Bacteriol.* **180**:4102–4110.
  50. Winstead, N. N., and A. Kelman. 1952. Inoculation techniques for evaluating resistance to *Pseudomonas solanacearum*. *Phytopathology* **42**:628–634.
  51. Yabuuchi, E., V. Kosako, I. Yano, H. Hotta, and Y. Nishiuchi. 1995. Transfer of two *Burkholderia* and an *Alcaligenes* species to *Ralstonia* gen. nov.: proposal of *Ralstonia pickettii* (Ralston, Palleroni and Doudoroff 1973) comb. nov., *Ralstonia solanacearum* (Smith 1896) comb. nov. and *Ralstonia eutropha* (Davis 1969) comb. nov. *Microbiol. Immunol.* **39**:897–904.
  52. Yamada, T., T. Kawasaki, S. Nagata, A. Fujiwara, S. Usami, and M. Fujie. 2007. Isolation and characterization of bacteriophages that infect the phytopathogen *Ralstonia solanacearum*. *Microbiology* **153**:2630–2639.
  53. Young, R. 1992. Bacteriophage lysis: mechanism and regulation. *Microbiol. Rev.* **56**:430–481.
  54. Ziermann, R., and R. Calendar. 1990. Characterization of the *cos* sites of bacteriophages P2 and P4. *Gene* **96**:9–15.